The Plastic Flow Field in the Vicinity of the Pin-Tool during Friction Stir Welding

An analysis of the displacements of wire markers in the flow field around a friction stir welding pin-tool supports a rotating plug flow model.

BY E.L. BERNSTEIN AND A.C. NUNES, JR.

ABSTRACT: The plastic flow field in the vicinity of the pin-tool during Friction Stir Welding (FSW) needs to be understood if a theoretical understanding of the process is to be attained. The structure of welds does not exhibit the flow field itself, but consists in a residue of displacements left by the plastic flow field. The residue requires analysis to extract from it the instantaneous flow field around the pin-tool.

A simplified merry-go-round model makes sense of some tracer experiments reported in the literature.

A quantitative comparison is made of the displacements of copper wire markers with displacements computed from a hypothetical plastic flow field. The hypothetical plastic flow field consists in a circular rotation field about a translating pin tool with angular velocity varying with radius from the pin centerline. A sharply localized rotational field comprising slip on a *surface* around the tool agreed better with observations than a distributed slip field occupying a substantial volume around the tool.

Both the tracer and the wire displacements support the "rotating plug" model, originally invoked for thermal reasons, of the FSW process.

E.L. BERNSTEIN is Associate Professor and Chair of the Department of Technology, Alabama A & M University, Huntsville, Alabama. A.C. NUNES, JR. is with the Materials, Processes, and Manufacturing Department at Marshall Space Flight Center, Huntsville, Alabama.

Introduction: The Rotating Plug Model and Its Thermal Motivation

Early attempts to model the Friction Stir Welding (FSW) process have raised questions about the nature of the flow field around the pin.

The simplest of our early models (Ref. 1) was a set of rotating ring elements interfacing between the rotating pin and a stationary workpiece. The shear stress between the elements was taken to depend upon temperature, but not shear rate; i.e. a plastic, not a viscous flow was taken to be appropriate for metallic deformation.

The outer ring surfaces have a larger area and a greater moment arm. Hence shear stress has to decrease with radial distance from the pin if the elements are to be in moment equilibrium. Since shear stress drops as temperature increases, mechanical equilibrium requires the temperature to rise with distance from the pin.

A temperature rising with distance from the pin would imply a temperature gradient for which the heat generated would flow backwards into the pin. Yet thermocouple measurements show a temperature falling with distance from the pin (at least outside the plastic zone) and indicate appreciable heat loss out to the plastic zone and into the workpiece. How could all this heat escape an equilibrium zone of plastic deformation if equilibrium requires a backflow of heat?

The alternatives were considered. Was it necessary to include a viscous term to stabilize the solution? This was rejected as inappropriate; metallic deformation is plastic, not viscous. Did the flow oscillate? Although some oscillations were observed, they were

thought to come from other causes. Nor were other researchers reporting oscillations. In the end oscillations were rejected. Had the wrong deformation field been assumed? An equilibrium solution could be obtained if the rotating ring elements were condensed to a single slip surface.

This would imply a plug of workpiece metal sticking to the pin and shearing against stationary workpiece metal over a cylindrical interface at some distance from the edge of the pin. Some tentative embedded thermocouple data received from the University of Texas at El Paso (UTEP) (Ref. 2) showing a very flat temperature in the vicinity of the pin seems to confirm the nondeforming plug of metal around the pin, for the temperature field should show a divergence where plastic flow is generating heat. No divergence implies no plastic flow, at least to the precision of the measurement.

At this point the rotating plug model illustrated in Fig. 1 was conceived (Ref. 3):

The primary metal flow in the friction stir welding process is conceived as a plug of metal rotating with the pin-tool. Shear occurs only (excluding secondary flow discussed below) over the encapsulating interface that separates the plug from the rest of the workpiece.

The movement of metal around the pin as the pin translates through the workpiece takes place by a LIFO (Last In First Out, a metaphor borrowed from the discipline of accounting) wiping action on the surface of the plug. What is successively wiped on, one influx over the other, on the forward interface is successively wiped off, top/last influxes first, on the trailing side.

But superimposed upon the primary plug rotational flow is a secondary circulation driven by threads on the pin and resembling a vortex ring wrapped around the pin . The secondary vortex ring circulation is conceived as much slower than the primary plug rotational flow. The primary plug rotational flow is taken to be the main power dissipation mechanism in friction stir welding, while the secondary vortex flow chiefly has the effect of moving metal in and out of the primary flow.

Do actual flow observations confirm the rotating plug model? Tracers observed in polished and etched sections of a weld represent a *residue* of displacements from a passing tool and not a snapshot of the instantaneous flow. The relation between metallographic observations and plastic flow patterns is not immediately obvious, but it may be extracted by analysis.

Primary Flow Features and The Merry-Go-Round Model

If the secondary flow is ignored, the main features of rotating plug flow may be visualized by the "merry-go-round" model illustrated in Fig. 2.

A marker particle embedded in the metal "walks up" to the plug, "steps on", is rotated round, and, if the plug rotation is rapid, the particle has little chance to move into the plug before it finds itself stepping off on the trailing side. It can be shown that the particle steps off at the same distance from the line of motion as it steps on.

Outside the merry-go-round

$$\text{for } x^2 + y^2 > r^2 \qquad dx = -V dt \qquad dy = 0 \qquad (1a,b,c)$$

And on the merry-go-round

$$\text{for } x^2 + y^2 \leq r^2 \qquad dx = -y\omega dt - V dt \qquad dy = x\omega dt \qquad (2a,b,c)$$

where x = coordinate from center of merry-go-round along the line of motion of the plug/merry-go-round, i.e. opposite the direction of "walking",

y = coordinate from center of merry-go-round perpendicular to the line of motion,

r = radius of merry-go-round,

ω = angular velocity of merry-go-round,

-V = velocity of markers, initially towards merry-go round, and

t = time.

Elimination of dt yields

$$x dx + \left(y + \frac{V}{\omega}\right) d\left(y + \frac{V}{\omega}\right) = 0 \tag{3a}$$

or, V and ω being constants, on the merry-go-round

$$x^2 + \left(y + \frac{V}{\omega}\right)^2 = \text{Constant} \tag{3b}$$

or, substituting $x^2 + y^2 = r^2$ for the condition at the edge of the merry-go-round,

$$r^2 + 2y\left(\frac{V}{\omega}\right) + \left(\frac{V}{\omega}\right)^2 = \text{Constant} \tag{4a}$$

or, at the edge of the merry-go-round,

$$y = \text{Constant} \tag{4b}$$

or

$$y_{on} = y_{off} \tag{4c}$$

Hence, applying the merry-go-round model to the friction stir welding plug, particles should get off the plug along the same line as they approached it! The trajectories on the merry-go-round are circles centered on a point at $x = 0$, $y = -\frac{V}{\omega}$ with a radius such that a trajectory intersects the boundary of the merry-go-round at the get-on and get-off points. Typical magnitudes of V/ω encountered in friction stir welding are on the order of 0.1 mm, so small that the trajectories of rotated metal particles remain essentially at the surface of the rotating plug with negligible penetration into the plug. Hence the presence of an impenetrable tool metal core does not affect the model, and the wiping-on and wiping–off conception of the mechanism by which metal is moved from the front to the back of the tool is justified.

K. Colligan's (Ref. 4) shot tracer patterns in plan view, i.e. the plane of the workpiece plate, frequently exhibit such a pattern: for example, positions 5,7,8,11,12 for 6061 aluminum and 5, 6, 8, 11 for 7075 aluminum. But sometimes the get-off point is displaced to one side or other perpendicular to the travel direction.

Positions 6, 9, 10 for 6061 aluminum or 9 for 7075 aluminum seem to exhibit premature exit from the rotational field. It is proposed that this is brought about by a downwards shift of the tracer into a region where the plug radius is smaller. That is, it is a secondary flow feature. Secondary flow features will be more fully discussed below.

Positions 1, 2, 3, 4 for 6061 and 1, 2, 3, 4, 7 for 7075 aluminum seem to exhibit excessive retention of tracer material (and late release) as well as considerable scatter. They occur towards the top of the pin, where the plug is further out and where, it is conjectured, the secondary flow tends to shift the tracer material back into the rotating plug. The scatter is presumed due to the reduced slope of the plug surface, so that small

tracer position variations result in relatively large variations in the radius of the plug encountered.

The middle of a line of people stepping up to a merry-go-round will be transported rapidly the entire diameter of the merry-go-round. The people at the edges will have to walk the entire diameter of the merry-go-round. (As was discussed above they will retain their relative places on the line.) The people at distances in between will be transported rapidly by the length of the chord of the merry-go-round circle in their way, $2\sqrt{r^2 - y^2}$. Thus after walking through the merry-go-round the center of the line will be displaced with respect to the unaffected regions of the line by Δx, such that

$$\Delta x = -2\sqrt{r^2 - y^2} \tag{5}$$

Note that the people shifted forward by the merry-go-round will retain their relative positions in the line. We have heard an argument against the transport of metal around the pin by the proposed plug wiping mechanism that states, "How do you explain the observed tendency for tracer metal to the left of the pin to remain on the left and that on the right to remain on the right? Wouldn't this require the flow to divide and flow around the pin in a kind of non-rotational extrusion process?" This argument loses its force, however, in the light of the above analysis, which shows how the wiping mechanism tends to produce this effect, too. The shot displacement experiments of K. Colligan show this tendency, but they also show violations of the tendency, which would be difficult for the extrusion model to explain.

In the tracer experiments of A.P. Reynolds *et al.* at the University of South Carolina (Ref. 5) a slab of tracer material perpendicular to the path of the pin-tool is bowed out by the encounter with the pin-tool into a shape like that of equation 5, as do tracer experiments that we have carried out at Marshall Space Flight Center. That is, the bowed shape is seen on the retreating side of the pin-tool. On the advancing side of the pin-tool a forward extending spur is seen. This is a secondary flow feature and will be explained below.

Secondary Flow Features

K. Colligan's observations deviate from the idealized patterns discussed above in that the trailing particle wakes may be linear but displaced or may be dispersed in a chaotic pattern. Sometimes there are two distinct particle trails, for example positions 9 and 10 for the 6061 aluminum and positions 4 and 9 for the 7075 aluminum. In Ref. 4 he remarks, "in those cases where the tracer material was chaotically deposited, the tracer material was also moved from its original depth and scattered through the thickness to a somewhat greater depth."

This implies an involvement of the secondary circulation. The postulated ring vortex secondary circulation wrapped around the pin-tool shifts tracers down close to the pin and up further out, outwards at the bottom, and inwards at the top just under the shoulder. Close to the pin the flow is downwards, impelled by the threads on the pin. Further out (around the middle of the pin) the flow is upwards.

The side-view radiographs of the Colligan tracers generally show a rise as the tracer passes the pin, as would be expected if the tracer is also passing through the outer portion of the secondary flow vortex. Positions just under the shoulder at the top of the pin are the ones showing the highest level of chaotic dispersion. These positions show *downward* displacements of tracers, as if the secondary vortex sweeps the tracers in and then down. The primary shear flow boundary spreads out from the pin in a flattened surface at the top of the pin just beneath the shoulder. Slight differences where tracer particles enter and leave the rapidly moving primary plug flow could well account for the observed chaotic scatter. The presumed low angle encounters just under the shoulder would make relatively large variations in radius possible.

The South Carolina paper traces deviate from the idealized patterns discussed above in that they also exhibit a spike in the direction of motion of the pin-tool

on the forward-moving side of the pin. The spike seems to be most pronounced in the upper portion of the plug, just under the shoulder where the radius of the plug changes rapidly from a value close to that of the pin radius to that at the edge of the shoulder. This is also a site at which the secondary upflow from the bottom of the pin turns in and begins the downward leg of the circulation. What happens if the secondary flow pushes tracer metal down the pin to locations where the radius of the slipping plug is substantially reduced?

On the merry-go-round if $\frac{V}{\omega}$ is small compared to r, the path of the tracer closely follows the outer edge of the merry-go-round in accordance with equation 4a. Typical values of $\frac{V}{\omega}$ are on the order of 0.1 mm while r is on the order of 5 mm. This would be consistent with a few percent reduction in trajectory radius within the merry-go-round, but the essential motion is around the circumference of the merry-go-round.

If the radius of the merry-go-round suddenly decreases, it retreats and abandons the particle that was on its periphery. The particle stops rotating but continues to move toward the merry-go-round ($dx = -Vdt$, $dy = 0$) until it can get back on. While it was on the merry-go-round it received a shift in position due to the rotation.

It receives a lateral shift Δy

$$\Delta y = y - y_o = \frac{r_o^2 - r^2}{2\left(\frac{V}{\omega}\right)} \approx \frac{r_o \omega}{V} \Delta r \tag{6}$$

where y_o = initial position on y-axis and
r_o = initial radius,

and a back shift Δx (against the direction of particle motion, the merry-go-round pivot considered fixed)

$$\Delta x = x - x_o = x_o \left(1 - \sqrt{1 - \frac{2\left(y_o - \frac{V}{\omega}\right)\Delta y + \Delta y^2}{x_o^2}} \right) \approx \frac{y_o}{x_o} \Delta y \tag{7}$$

where x_o = initial position on x-axis.

In Fig. 1 it is to be noted that the while the primary flow takes a tracer particle around the plug, the secondary flow can move a tracer particle into and out of the primary flow. In particular, this happens at the top of the pin.

Suppose that

$$V = 3 \text{ mm/sec}$$

$$\omega = 300 \text{ RPM}$$

$$p = 1 \text{ mm}$$

where p is the pitch of the threads on the pin-tool. The downwards speed of the metal at the pin surface, say 3mm radius, is then 300 mm/min or 5 mm/sec. The outer portion of the secondary flow vortex presumably has a velocity on the order of 5 mm/sec. We imagine the outer streamline of the secondary flow (See Fig. 3) entering the rotating plug at the

edge of the shoulder, say 9 mm radius, and descending down the pin-tool surface, but the inner streamlines enter and leave.

Let us say one streamline enters the plug at 8 mm and leaves at 5 mm. The time in the plug will be on the order of 3/5 or 0.6 seconds. This is plenty of time for the plug to impart a full rotation to the particles moving along this streamline. A full rotation takes 1/300 min ute or 0.2 seconds.

Let us say another streamline enters at 6.55 mm and leaves at 6.45 mm . It remains in the plug for 0.1/5 or 0.02 seconds, only enough for 0.1 rotations or 36°. then

$$\Delta x = 3.82 \text{ mm}$$

$$\Delta y = 1.24 \text{ mm}$$

and from equation 6, the effective radial distance change due to plug motion is

$$\Delta r = -0.018 \text{ mm}$$

This radial distance is enough less than the 0.1 mm so that it may be ignored to an order of magnitude approximation. If the effective radial distance change due to plug motion were larger, it would cut down the effect by causing the tracer to jump off the translating band of metal sooner.

It can be seen, and this is the point of the above example, that a spur of segregate will be displaced forward (i.e. in the direction of pin-tool translational motion) on the advancing side of the of the pin-tool given the assumptions made.

Wire Tracers - Experimental Procedure

The idea to use wire tracers was conceived when it was found (Ref. 2) that thermocouples were not necessarily destroyed by an encounter with the friction stir welding pin-tool. A pair of test plates 8.13 mm thick of 2195 aluminum-lithium alloy were prepared for welding as flollows.

Eight copper wires, 0.71 mm in diameter, were embedded in holes drilled into the contact surfaces of the weld perpendicular to the weld. Four wires were placed on each side of the weld at four different levels in the plate, 0.48, 3.02, 5.56, and 7.65 mm from the top surface of the plate.

The contact surface were butted together, the plates securely clamped, and a friction stir weld was run down the seam at 250 RPM and 1.48 mm/sec.The pin length was 6.86 mm and the diameter, 11.84 mm.

A radiograph of the friction stir welded plates is shown in Fig. 4. Superimposed on the radiograph are retreating-side wire contours computed for varying shear distribution profiles. The sharpest, most plug-like distribution agrees best with the empirical results.

Wire Tracers - Analysis

The general appearance of the wire tracers resembles that of the inserted slab markers of Reynolds *et al.* (Ref. 5). The retreating side shows a loop extending to the rear. The advancing slide shows a forward-displaced spur at the edge of the plastic zone and, further into the plastic zone, the loop extending to the rear.

Let it be noted that here "plastic zone" means the cross sectional region of the weld where metal is subjected to substantial irreversible plastic deformation. In the moving plug model of friction stir welding the *primary* plastic deformation takes place only over a *surface* of cylindrical symmetry bounding a plug of metal moving with the pin-tool. The occurrence of plastic flow over a *surface* and the generation of a *volume* of plastically

deformed metal are two different things and do not conflict. The surface of plastic deformation around the pin, however, as it moves through the workpiece, does determine the outer envelope or boundary of the plastic zone. Hence the plug shear boundary should be a surface of revolution with the outer contour that of the boundary of the plastic zone on the weld cross section.

If the break points at which the wire begins to bend are taken as points where plastic zone begins, it is possible to plot the boundary of the plastic flow field around the pin-tool. This is done in Fig. 5.

The plastic zone estimated from the wire markers starts approximately at the edge of the shoulder and moves in to enfold the pin.

There appears to be an inflection point between the upper 2 points and the lower 2 points on each side of the seam. Possibly it separates flow dominated by the shoulder from that dominated by the pin.

If the pin is missing, a shoulder alone produces a plastic zone that extends down into the workpiece (Ref. 6). Extrapolation of the plastic zone bounded by the four points closest to the shoulder suggests that it would extend to a depth of the order of 5 mm, or about 20% of the shoulder diameter. Presumably pins appreciably shorter than 5 mm would not affect the plastic zone. For longer pins, both pin and shoulder create boundary conditions that establish the contours of the slip surface.

The theoretical determination of this surface has been proposed (Ref. 3) as a problem in the calculus of variations: the minimization of torque. The easiest to slip surface should slip first and prevent the further rise of torque and the slip of other, more difficult to slip surfaces, but the solution is complicated by the necessity to couple into the situation the temperature field which is generated by the slip. Treatment of this problem is outside the intended scope of this paper. It is planned to deal with the dynamics of the torques and forces in friction stir welding in a subsequent paper.

A row of unconnected marker particles in a moving vortex field would receive displacements in accordance with equation 2. Relative to the plate, where vortex field $\omega(r)$ is centered on position ξ on the x-axis along which it moves with velocity V, the particle displacements are:

$$dx = -y\left(\frac{\omega(r)}{V}\right)d\xi \tag{8}$$

$$dy = (x-\xi)\left(\frac{\omega(r)}{V}\right)d\xi \tag{9}$$

where radius from the center of the vortex field is given by

$$r = \sqrt{(x-\xi)^2 + y^2} \tag{10}$$

For plug type rotation $\omega(r)$ is a step function. The angular velocity Ω of the pin-tool within the plug drops to 0 suddenly at the edge of the plug. A more general distribution can be represented by the expression:

$$\omega(r) = \frac{\Omega}{1 + \left(\frac{r - r_{pin}}{r_{plug}} \right)^N} \tag{11}$$

for $r \geq r_{pin}$

where r_{pin} = pin radius
r_{plug} = plug radius
N = parameter determining steepness of step.

When N is small, the step is gradual. When N is large, the step is steep, approaching plug type rotation. Some plots of this function are exhibited in Fig. 4. It should be understood that the distributed, low N fields represented by this distribution will not in general be in equilibrium. This doesn't matter for the present concerns, which are purely kinematic.

But wire tracers are not the same as lines of disconnected particles. Disconnected particles may be expected to yield loops on the trailing side of the weld with a displacement approximating to the $-2\sqrt{r^2 - y^2}$ of equation 5. A maximum displacement on the order of the diameter of the merry-go-round or plug diameter should be observed.

Suppose the merry-go-round model is changed such that the particles moving toward the merry-go-round are all connected by a rope. Let us also suppose that the line of particles only extend to the centerline of motion like the experimental wires. Whereas the first particle of a disconnected line to encounter the merry-go-round is rapidly whisked to the other side of the merry-go-round, the first particle of a connected line is held back. It slides on the floor of the merry-go-round as the friction between it and the merry-go-round floor is inadequate to overcome the pull of the rope. A schematic of the way the wire is deformed by the passage of the pin-tool according to the plug rotation model is shown in Fig. 6.

As each successive particle gets on the merry-go-round it is swept around until the connecting rope is approximately parallel to the direction of primary motion around the merry-go-round center. A train of particles develops forming an arc around the periphery of the merry-go-round pinned in place by its connection with the external particle line. When the pinning connection passes the center of the merry-go-round no more particles can enter the merry-go-round and the approximately circular arc of connected particles slips off the merry-go-round. A maximum displacement on the order of the radius, not the diameter, of the merry-go-round or plug diameter should be observed. In Fig. 7 circles corresponding to the diameters of the plastic zone shown in Fig. 5 have been superimposed over the wire markers. It is noteworthy that the stress on the wire has been sufficient to produce fractures in the wire, particularly on the advancing side.

Although the copper wire flow stress is higher than that of the aluminum-lithium alloy matrix, the assumption used in the computation that the wire does not extend, but merely bends is not exactly true. Nevertheless this assumption is substantially better than assuming a train of disconnected particles and is taken to be good enough for present purposes.

Let us consider an element of a wire extending from x_{i-1}, y_{i-1} to x_i, y_i. The displacement of the ith point is that at the (i-1)th plus a rotation. Assuming an angular velocity Ω, the displacements $\delta x_i . \delta y_i$ of the ith point in time δt are given by

$$\delta x_i = \delta x_{i-1} - (y_i - y_{i-1})\Omega\delta t \tag{12}$$

$$\delta y_i = \delta y_{i-1} + (x_i - x_{i-1})\Omega\delta t \tag{13}$$

Ω is assumed to be equal to the local rotation. A unit vector $\hat{u}$ perpendicular to the wire segment is given by

$$\hat{u} = \frac{-(y_i - y_{i-1})\hat{i} + (x_i - x_{i-1})\hat{j}}{\sqrt{(y_i - y_{i-1})^2 + (x_i - x_{i-1})^2}} \tag{14}$$

The velocity of the flow field at the ith end of the wire segment is

$$\bar{V}_i = -y_i\omega(r_i)\hat{i} + (x_i - \xi)\omega(r_i)\hat{j} \tag{15}$$

and for the (I-1)th end

$$\bar{V}_{i-1} = -y_{i-1}\omega(r_{i-1})\hat{i} + (x_{i-1} - \xi)\omega(r_{i-1})\hat{j} \tag{16}$$

Equating the flow rotation to the wire segment rotation

$$\bar{V}_i \cdot \hat{u} - \bar{V}_{i-1} \cdot \hat{u} = \sqrt{(y_i - y_{i-1})^2 + (x_i - x_{i-1})^2}\,\Omega \tag{17}$$

$$\Omega = \frac{(y_i - y_{i-1})\left[y_i\omega(r_i) - y_{i-1}\omega(r_{i-1})\right] + (x_i - x_{i-1})\left[(x_i - \xi)\omega(r_i) - (x_{i-1} - \xi)\omega(r_{i-1})\right]}{(y_i - y_{i-1})^2 + (x_i - x_{i-1})^2} \tag{18}$$

Note that if $\omega(r_i) = \omega(r_{i-1}) = \omega$, the case for solid body rotation, then $\Omega = \omega$.

Equations 12, 13, and 18 provide a basis for a finite difference computation of the evolving shape of a wire in the plastic flow field around a friction stir welding pin-tool.

For quasi-equilibrium wire deformation $\Omega = 0$. If the position of the (I-1)th node is known, x_{i-1}, y_{i-1}, and if the length of the segment between the (i-1)th and the ith node, $\sqrt{(y_i - y_{i-1})^2 + (x_i - x_{i-1})^2}$, is known, equation 18 completes the information needed to determine the position of the ith node.

Conclusions

The trajectories of particle tracers in the form of inserted slabs or disconnected shot or connected wires in the vicinity of a friction stir welding pin-tool are intelligible in the context of the rotating plug model of the flow field. In this model the plastic flow occurs as (1) a primary plug rotation about the pin-tool with shear occurring only on the cylindrical surface separating the plug from the workpiece and (2) a secondary vortex ring flow driven by threads on the pin-tool and superposed upon the primary plug rotation flow.

The back-looping of the tracer behind the pin-tool is a result of the primary plug flow. The origin of this feature can be understood by visualizing particles marching up to a merry-go-round.

The forward-directed spur on the advancing side of the pin-tool can be understood as an effect of the secondary flow introducing particles into the rotating plug and rapidly extracting them so that the plug rotation only has time to impart a forward shift to them and cannot rotate them fully around to the rear of the plug.

When computations were made of the shapes of wires deformed in spatially extended primary flows, agreement with observations was best when the the flow angular velocity was constant up to a critical radius and then dropped off precipitously, i.e. as the rotating plug model would have it.

Acknowledgements

This effort was partially supported by the NASA Summer Faculty Research Program. The authors are greatly indebted to R.A. Venable of Lockheed Martin Corporation, who designed the experimental plate, executed the weld, incorporated the experimental data into the computer, and provided valuable advice. K. Colligan kindly read this paper and made suggestions which have been incorporated into the paper.

References

1. Nunes, A.C., Jr., 1997. Friction Stir Welding Process Analysis: A Progress Report. *Proceedings of Friction Stir Welding Workshop.* Marshall Space Flight Center, February 24.

2. McClure, J.C. 1998. A Thermal Model of Friction Stir Welding. Presentation at Marshall Space flight Center.

3. Nunes, A.C., Jr., Stewart, M.B., Adams, G.P.,and Romine, P. A Combined Experimental and Analytical Modeling Approach to Understanding Friction Stir Welding. Submitted to *Journal of Materials Processing & Manufacturing Science.*

4. Colligan, K. 1999. Material Flow Behavior during Friction Stir Welding of Aluminum. *Welding journal* 78(7): 229-s to 237-s.

5. Reynolds, A.P., Seidel, T.U., Simonsen, M. 1999. Visualization of Material Flow in an Autogenous Friction Stir Weld. *International Symposium on Friction Stir Welding, Rockwell Science Center, Thousand Oaks , California.*

6. McClure, J.C. 1998. Private Communication.

Figure Captions

Fig. 1 -- A centerline section of the rotating plug of the friction stir welding process showing the principal metal flows as conceived in the rotating plug model. It is a side view under conditions of negligible tool translation velocity when the sides are not differentiated. The primary flow consists in the rotation of a plug of metal with respect to the workpiece. The primary shear takes place over a surface of cylindrical symmetry about the pin-tool. There is also a secondary flow in the shape of a vortex ring directed downwards at the pin surface and flowing back up at a distance further out.

Fig. 2 -- In the merry-go-round model tracer particles step on and off the rotating plug symmetrically. The rapid rotational transport advances a particle by the length of the chord of the merry-go-round circle in negligible time to cause a bulge in the emerging line.

Fig. 3 -- A centerline section of the rotating plug (as in Fig. 1) focussing on the corner between pin and shoulder showing hypothetical streamlines in the secondary flow beneath the shoulder. The streamline towards the center of the pattern transports particles in and out of the revolving plug in a very short time interval; during this time interval a particle moving along this streamline is transported a short distance almost tangential to the rotational velocity. This is proposed as the origin of the spur of forward-displaced material on the advancing side of the pin.

Fig. 4 – Radiographs of copper wire markers on retreating side of friction stir weld (heavy lines – compare with Figure 7). Superimposed are computed wire shapes (multiple lighter lines) for different angular velocity/shear distribution profiles characterized by parameter N. The effect of parameter N is shown in the plot above of angular velocity vs. radial distance from the pin centerline for a plug radius of approximately 1.00 inch. The sharpest, most plug-like distribution (largest N) agrees best with the empirical results.

Fig. 5 -- Plot of the plastic shear zone around the pin-tool from the locus of points at which the wire markers begin to bend.

Fig. 6 – Wire deformation process schematic. a) Wires entrained in rotating plastic zone. b) Plastic zone moves past wire on retreating side. Wire on advancing side fractures. Fractured wire segment rotates with plastic zone until zone moves on past it. c) Resultant wire configuration. The forward motion of the advancing side allows more time for the shift of metal by the secondary flow. Hence superimposed on the simple picture of this figure one would expect the apparent reduction in the radius of the plastic zone on the advancing side, which Figures 5 and 7 exhibit.

Fig. 7 -- Radiograph of a friction stir weld incorporating copper wire markers. Superimposed are plastic zone boundaries and the pin cross section. Apparent interference with the pin is attributed to activity under the pin (smallest circle) or transport of broken material around the pin (the radiograph is made after the pin has passed by) or experimental error (principally third circle from right on advancing side).

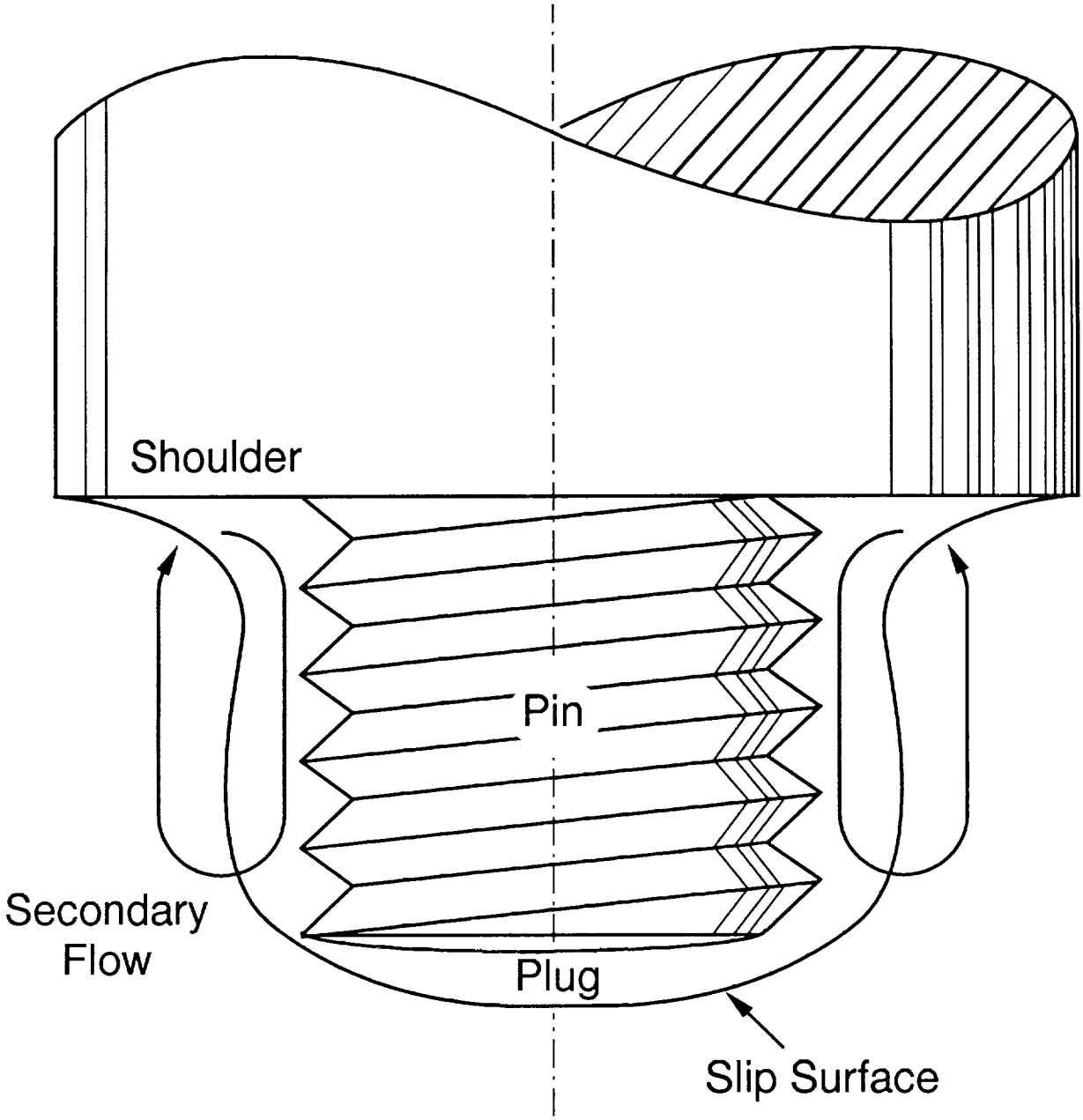

5-34243a(fig 1)

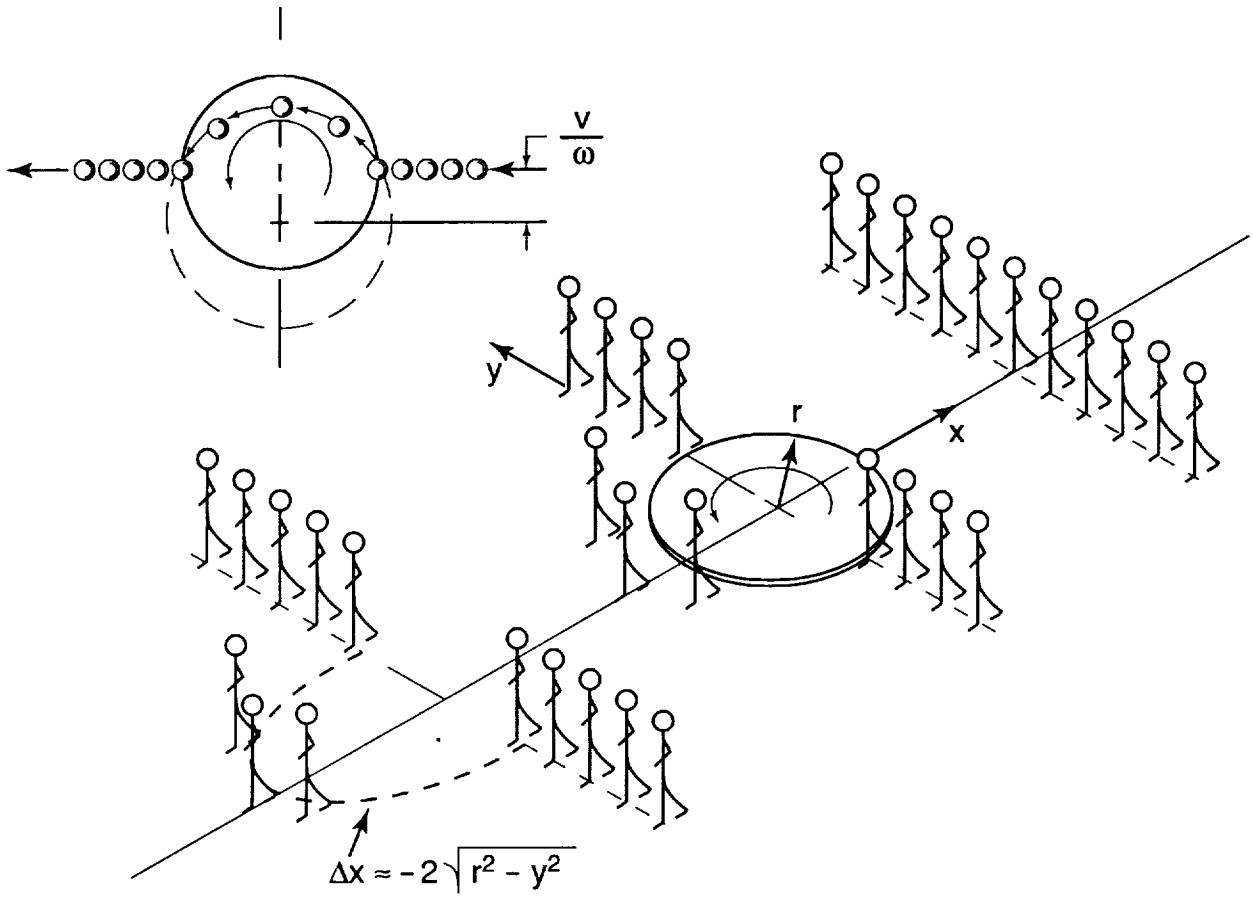

5-34243b(fig2)

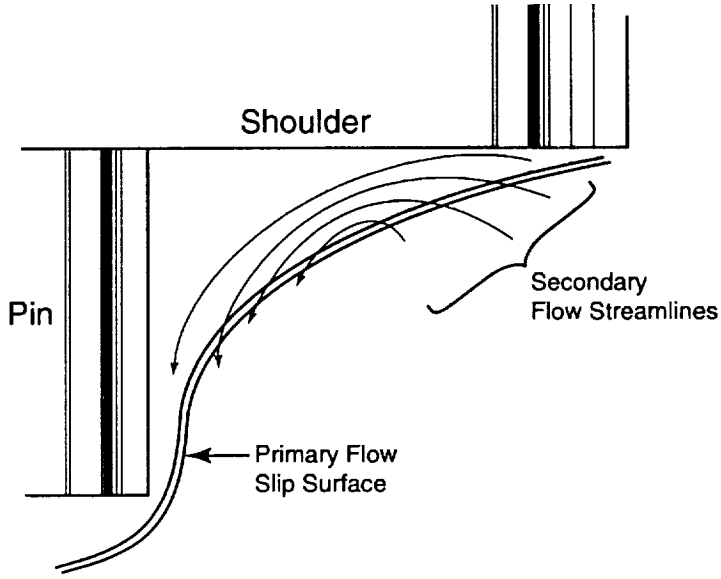

5-34243c(fig3)

Effect of Parameter N on Angular Velocity/Shear Distribution

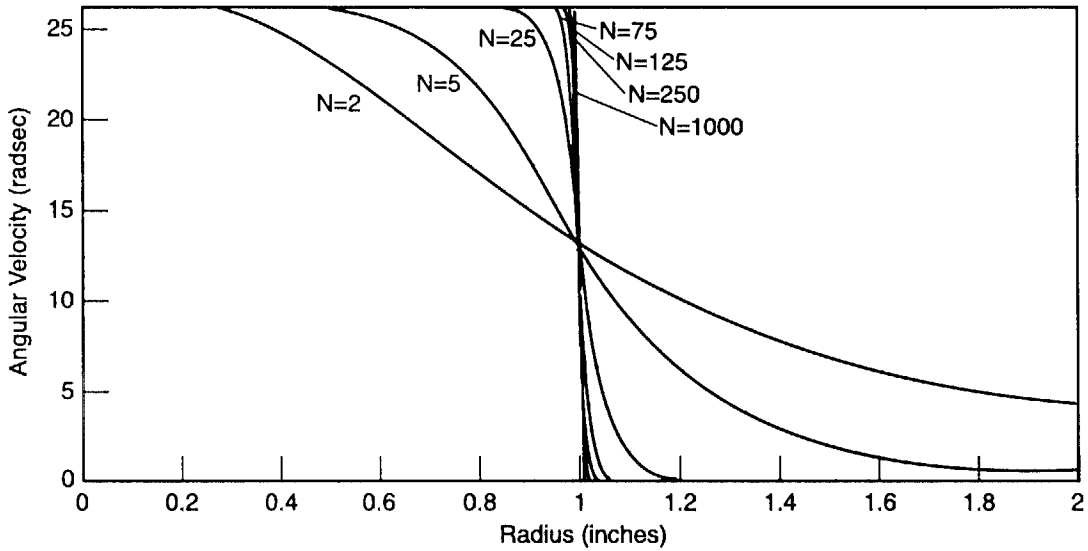

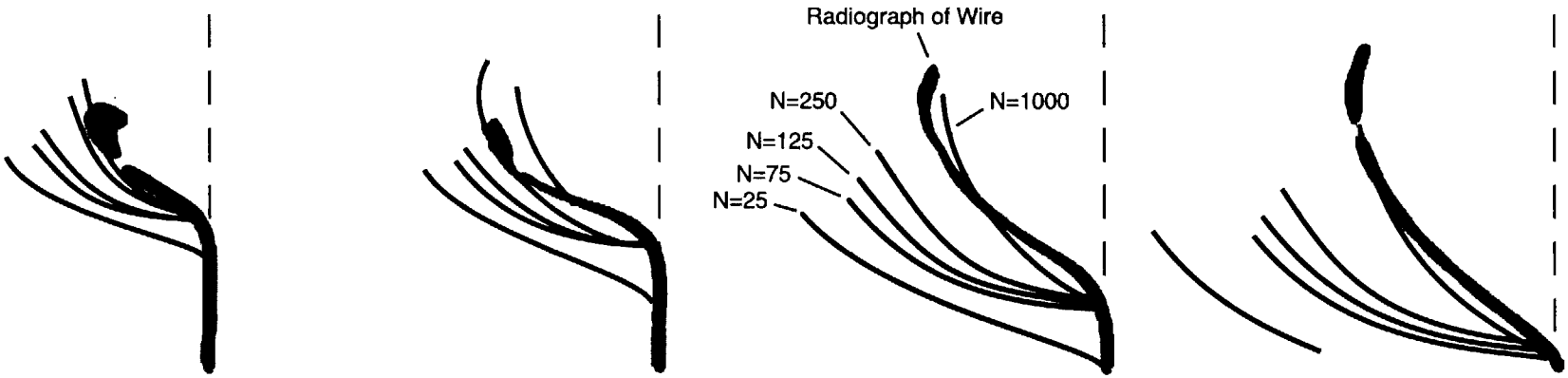

Computed Curves vs. Radiographs

5-34243d.fig4

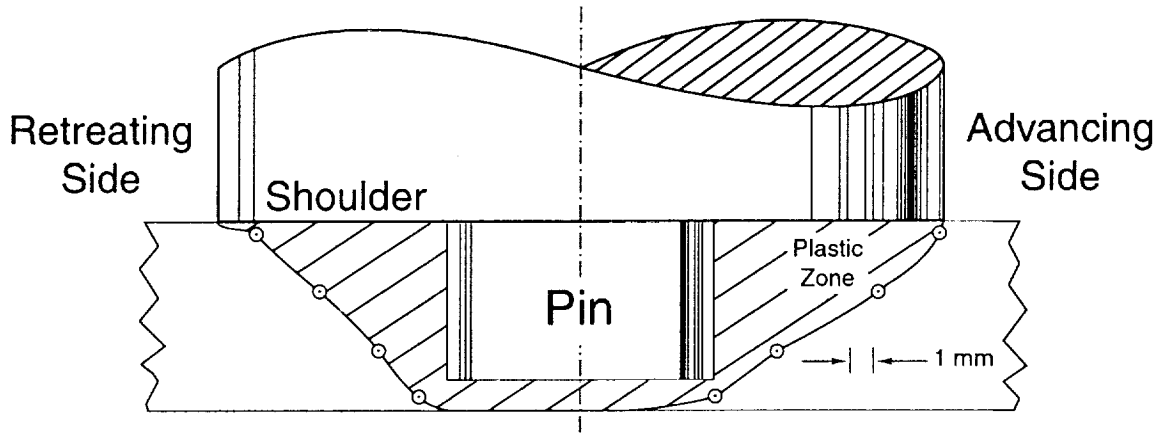

5-34243e.fig5

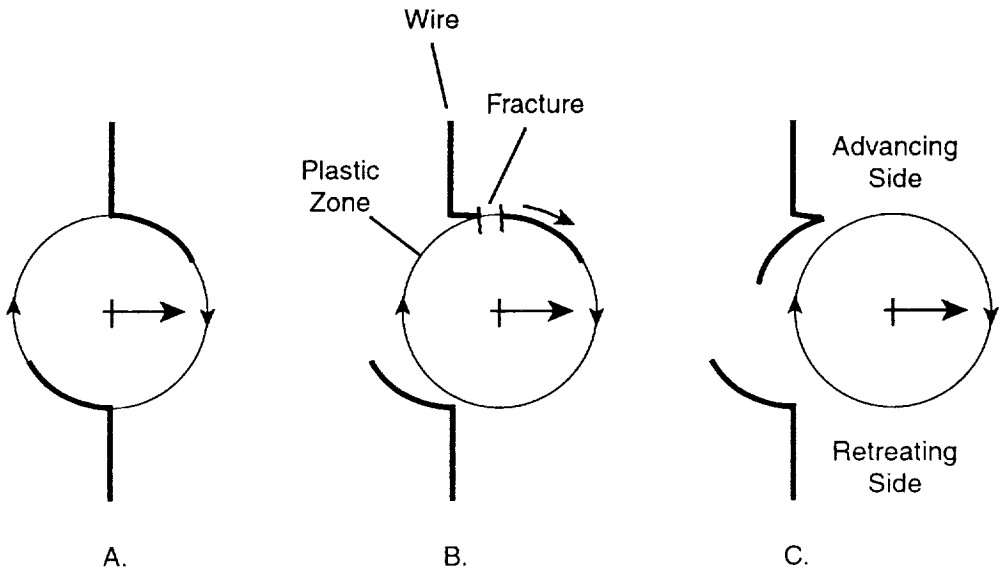
Wire
Fracture
Plastic
Zone
Advancing
Side
Retreating
Side
A.
B.
C.

Fig. 6

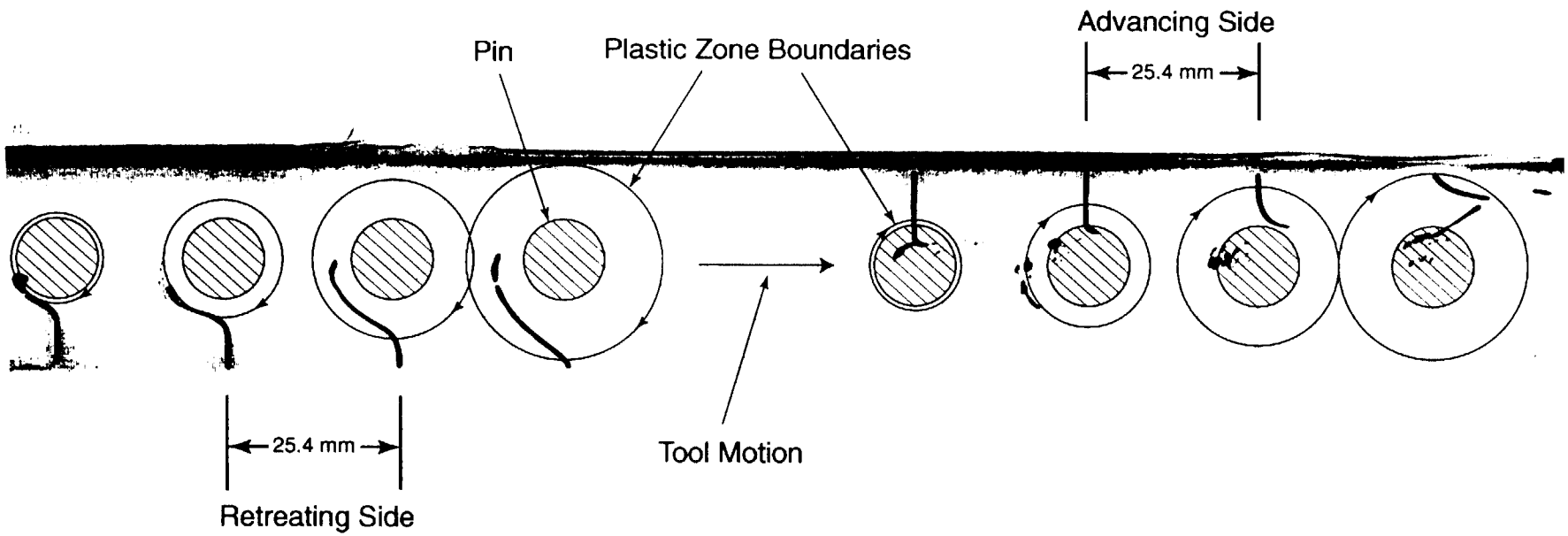

5-34243f(fig7)